Review Article
https://doi.org/10.5115/acb.2019.52.1.17
pISSN 2093-3665 eISSN 2093-3673
Anatomy & Cell Biology acb

Clinical anatomy of the maxillary sinus: application to sinus floor augmentation

Joe Iwanaga[1,2,3], Charlotte Wilson[1], Stefan Lachkar[1], Krzysztof A. Tomaszewski[4], Jerzy A. Walocha[5], R. Shane Tubbs[1,6]

[1]Seattle Science Foundation, Seattle, WA, USA, [2]Dental and Oral Medical Center, [3]Division of Gross and Clinical Anatomy, Department of Anatomy, Kurume University School of Medicine, Kurume, Japan, Departments of [4]Anatomy and [5]Medical Education, Jagiellonian University Medical College, Krakow, Poland, [6]Department of Anatomical Sciences, St. George's University, St. George's, Grenada, West Indies

Abstract: The anatomy of the maxillary sinus, especially its vascular anatomy, and its relationships with the teeth and alveolar processes have been well documented. The development of cone-beam computed tomography has resulted in dentists being more familiar with maxillary sinus floor augmentation procedures. This paper aims to revisit the classic anatomy of the maxillary sinus and review the newly published literature in order to help dentists diagnose in more detail and perform safer surgery of the maxillary sinus.

Key words: Anatomy, Cadaver, Maxillary sinus, Sinus floor augmentation, Maxillary artery, Dental implants

Received September 18, 2018; Revised October 10, 2018; Accepted October 21, 2018

Introduction

The maxillary sinus (MS), one of the paranasal sinuses first identified by ancient Egyptians, has been well studied, especially its structure, vascular anatomy, and relationship with the teeth [1]. Since the introduction of cone-beam computed tomography (CBCT) into clinical practice, sinus floor augmentation (SFA) has become more popular. This approach requires the knowledge of the surrounding structures that might be seen in the CBCT images. However, most of these structures which have been shown in computed tomography (CT) images are hard to understand due to its complicated morphology. Therefore, the aim of the current paper is to review the clinical anatomy of the MS for a better understanding of SFA procedures with several cadaveric images which could help understand the structures three dimensionally.

Corresponding author:
Joe Iwanaga
Seattle Science Foundation, 550 17th Ave, James Tower, Suite 600, Seattle, WA 98122, USA
Tel: +1-2067326500, Fax: +1-2067326599,
E-mail: joei@seattlesciencefoundation.org

Anatomy

Embryology

The MS begins to form during the 10th week of development. The mucosa located at the deeper anterior end of the ethmoid infundibulum presents invaginations toward the surrounding mesenchyme [2]. These invaginations fuse during the 11th week of development, giving rise to a single cavity representing the primordium of the MS [2]. The primordial shape of the sinus is characterized as an oval cavity with smooth walls [2]. Rapid growth of the MS has been observed during two periods of development: from the 17th to the 20th week and from the 25th to the 28th week.

Ossification of the sinus begins during the 16th week of development, beginning in the lateral wall of the sinus and spreading to the anterior wall by the 20th week, and to the posterior wall by the 21st week. The medial wall shows signs of ossification by the 37th week of development [2].

The floor of the sinus is related to the roots of the first premolar teeth at age 4 years and the second molar teeth at age

five years, and may extend to the third molar teeth and/or to the first premolar teeth, and sometimes to the canine teeth [3, 4].

Structure

The MS is pyramidal in shape and is the largest of the paranasal sinuses [3]. The anterior wall of the MS is formed by the facial surface of the maxilla and is internally grooved by the canalis sinuosus (which houses the anterior superior alveolar nerve and vessels) [3]. The anterior wall as three major landmarks: (1) the thin canine fossa; (2) the infraorbital foramen located in the midsuperior region; and (3) the infraorbital groove [3, 5, 6].

The posterior wall is formed by the infratemporal surface of the maxilla [3]. It forms the anterior border of the pterygopalatine fossa [5].

The superior wall is formed by the fragile, triangular orbit floor, with the infraorbital groove running through it [3, 6]. The roof of the sinus thickens toward the orbital margin, with a mean thickness of 0.4 mm medial to the infraorbital canal and 0.5 mm thick lateral to it [4].

The medial wall of the MS separates the sinus from the nasal cavity [6]. It is smooth on the sinus side and carries the inferior nasal conchae on the nasal side [3, 6]. The medial wall is rectangular in shape and is slightly deficient at the maxillary hiatus [3]. This opening is partially closed in an articulated skull by sections of the inferior turbinate, the uncinate process of the ethmoid bone, the perpendicular plate of the palatine bone, the lacrimal bone, and the overlying mucosa to form the ostium (Fig. 1) as well as anterior and posterior fontanelles [3, 5]. The ostium opens into the inferior part of the ethmoidal infundibulum, passing through the semilunar hiatus, then finally into the middle nasal meatus [3]. The ostium is elliptical-shaped throughout prenatal development and located in the anterior third of the ethmoidal infundibulum [2]. In adults, however, the ostium is located between the middle and posterior thirds of the ethmoidal infundibulum and tends to be positioned closer to the roof of the sinus than the floor [2, 3]. In some cases, the ostium is divided into two sections via a mucosal membrane [4].

The lateral apex of the MS extends into the zygomatic process of the maxilla and can reach the zygomatic bone therefore forming the zygomatic recess (Fig. 2) [3].

The floor of the sinus is formed by the alveolar and palatine processes of the maxilla and lies below the nasal cavity [3, 5], which is usually located from the mesial part of the first premolar to the distal part of the third molar with the lowest at the first and second molar (Fig. 3). The floor of the sinus is separated from molar dentition by a thin layer of compact bone [5]. The maxillary posterior teeth root tips are in close relation to the floor of the sinus, with the root tips of the molar being closer to the floor of the sinus than the premolars [7]. CT studies have revealed the mean distance between the maxillary posterior teeth and the sinus floor to be 1.97 mm [7]. CT studies have also shown that the roots of the first and second molars have been shown to have a significantly close relationship with the sinus floor in 40% of cases, and perforate the sinus floor in 2.2% and 2.0% of cases, respectively [4, 8].

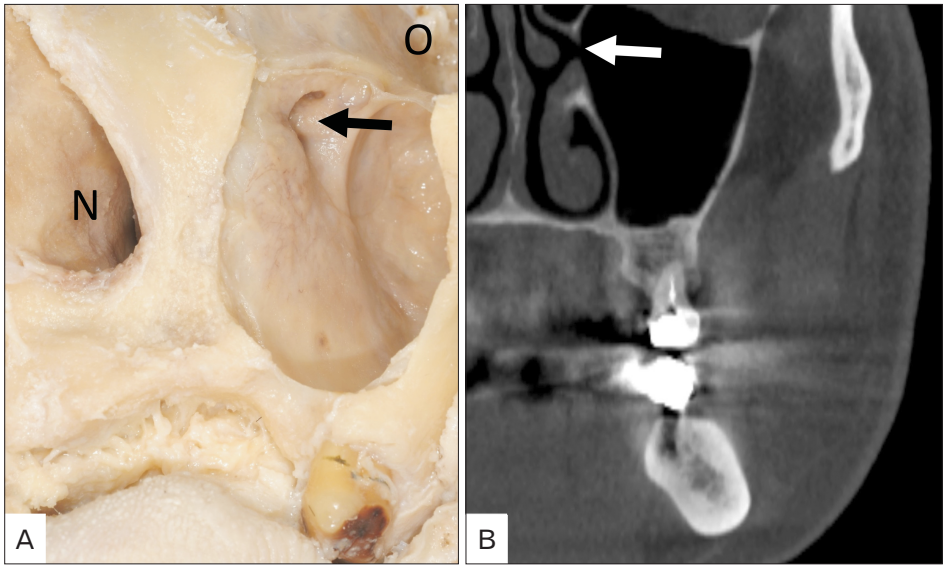

Fig. 1. Ostium on the left maxillary sinus (arrows). (A) Cadaveric dissection (anterolateral view). (B) Computed tomography (coronal image). N, nasal cavity; O, orbit.

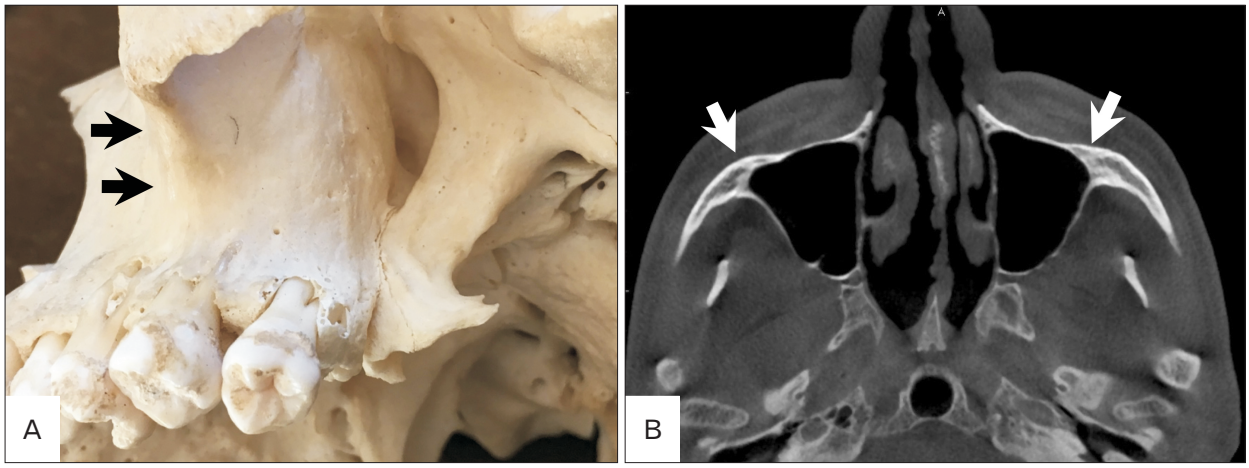

Fig. 2. The maxillary sinus extending into the zygomatic process (arrows). (A) Dry skull (inferolateral view). (B) Computed tomography (axial image).

Fig. 3. Relationship between teeth and maxillary sinus (right side). Note the root of the first premolar (arrow) is located most medially.

The palatal root of the first premolar tends to have the longest distance from the sinus floor whereas the second molar buccodistal root tip has the shortest distance to the MS floor [7-9].

Many CT studies have been conducted on the prevalence of septa within the MS, with results varying from 16% to 58% [10-12]. Complete partition of the MS is rare with reports of prevalence between 1.0% to 2.5% of cases [3, 4]. Two different types of septa have been identified. Primary septa are congenital, arising from maxillary development, and are above the teeth [13]. Secondary septa are acquired, arising from irregular pneumatization of the sinus floor after tooth loss [11]. Both primary and secondary septa can be found above an edentulous ridge [13]. The location of septa can vary. Prevalence of septa found in the anterior region (above the premolar teeth) ranges from 17.5% to 70% [11, 14]. Prevalence of septa found in the middle region (above the first and second molar teeth) range from 41% to 65% [13, 15, 16]. Prevalence of septa found in the posterior region (distal aspect of the second molar tooth) is found to be 22.5% to 22.7% [13, 14]. The height of septa ranges from 2.5 mm to 6.0 mm [9]. Cone beam CT studies have also revealed that septa in edentulous cases is more prevalent (27.7%) than in dentate cases (14.0% to 19.3%) [11, 13]. Clinical and anatomical studies have shown that the height of septa is greater in dentate cases than in edentulous cases. The average septa height in dentate cases has been reported at 12.2 mm whereas edentulous cases (total and partial edentulous) has a mean septa height of 8.06 mm [11].

The inner lining of the MS lacks periosteum and is therefore covered solely in mucus-producing ciliated pseudostratified columnar epithelium, with a higher density of cilia closer to the ostium [3, 9, 17]. Because the ostium tends to be located more superiorly along the medial wall of the sinus, mucous drainage relies heavily on the mucociliary escalator, with the cilia of the sinus beating towards the ostium [3].

Blood supply

Vascular supply to the MS is derived primarily from branches of the maxillary artery: the posterior superior alveolar artery, the infraorbital artery, and the posterior lateral nasal artery [3, 18, 19]. The posterior superior alveolar artery (PSAA) can course along the medial wall of the sinus [19]. The infraorbital artery passes along the infraorbital groove and canal, under the orbit, and finally through the infraorbital foramen on the facial surface of the maxilla [19]. The PSAA

https://doi.org/10.5115/acb.2019.52.1.17

(Fig. 4) and the infraorbital artery anastomose along the anterolateral wall of the sinus, supplying the mucous membrane of the nasal chambers [3, 18]. An extraosseous anastomosis often exists between these two arteries [3]. The posterior lateral nasal artery branches from the sphenopalatine artery and passes through the sphenopalatine foramen to enter the nasal cavity and can be found within the medial wall of the sinus [19]. As it continues anteriorly, the posterior lateral nasal artery begins to branch, supplying blood to the posterior and medial wall of the sinus [19].

Innervation

The MS receives general sensation innervation from the infraorbital and anterior, middle, and posterior superior alveolar branches of the maxillary nerve (V2) [3]. Most sensory innervation is provided by the posterior superior alveolar branch [5], which usually has two to three branches (Fig. 5). The anterior superior alveolar branch innervates the anterior portion of the MS, whereas the middle superior alveolar branch contributes secondary mucosal innervation. The ostium of the maxilla is innervated by the greater palatine nerve while the infundibulum is innervated by the anterior ethmoidal branch of the ophthalmic nerve (V1). Parasympathetic secretomotor fibers originate from the nervus intermedius of the facial nerve, synapsing in the pterygopalatine ganglion and proceeding to the sinus mucosa via the trigeminal sensory branches [5].

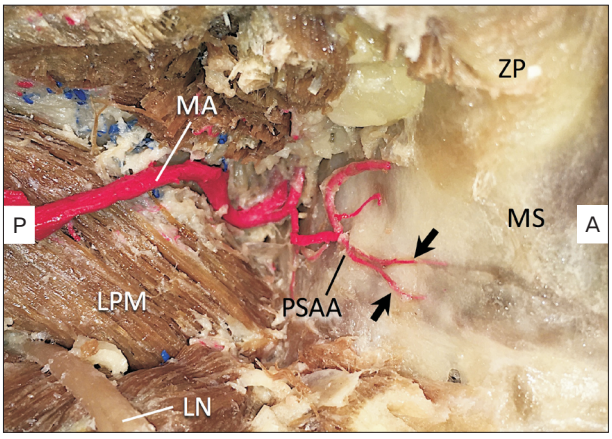

Fig. 4. Course of the right posterior superior alveolar artery. Note the two branches of posterior superior alveolar artery enter the posterior wall of the maxillary sinus (arrows). LN, lingual nerve; LPM, lateral pterygoid muscle; MA, maxillary artery; MS, maxillary sinus; PSAA, posterior superior alveolar artery; ZP, zygomatic process.

Age change

At birth, the MS measures <7.0 mm in anteroposterior depth, <4.0 mm in height, and <2.7 mm in width [5]. The height of sinus development depends on several factors: pressure from the eyeball against the orbit wall, the traction on the inferior portion of the maxilla by the facial muscles, and the eruption of permanent detention [4, 6].

The MS grows most rapidly between ages 1 and 8 years, growing laterally past the infraorbital canal and inferiorly to the middle aspect of the inferior meatus [5]. At age three years, the downward pull of the facial muscles continues to pull on the maxillary bones [6]. The roof of the sinus presents a more inferolateral position in childhood, before assuming its more horizontal position in adulthood due to progressing pneumatization [5]. The floor of the sinus lies somewhat lower than the insertion of the inferior nasal conchae at the

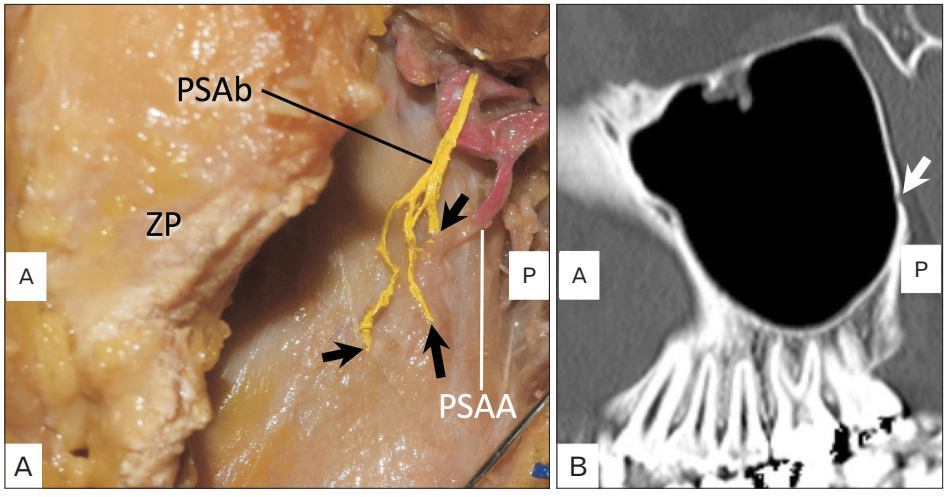

Fig. 5. Course of the left posterior superior alveolar branch of the maxillary nerve. Note the three branches enter the posterior wall of the maxillary sinus (arrows). (A) Lateral view of the posterior superior alveolar branch of the maxillary nerve (PSAb) in the cadaveric dissection (left side). (B) Computed tomography (sagittal image). A, anterior; P, posterior; PSAA, posterior superior alveolar artery; ZP, zygomatic process.

end of the second year of life [4]. The floor lies at about the height of the inferior nasal conchae at age seven years, and at the level of the floor of the nasal cavity at age 9 years. In some cases, the floor of the sinus can continue further into the hard palate in the medial direction, creating the palatine recess [4].

Primary dentition does not have an influence on the growth of the MS due to dental follicles of primary dentition being separated from the floor of the sinus via a thick layer of bone, ranging from 1.5 to 2.0 mm in thickness [4]. From ages 6 to 11 years, almost all tooth buds that are lateral to the incisors lie in immediate relation to the mucosa of the MS [4]. The MS reaches its adult size between 18 and 21 years of age with the eruption of the third molars [8]. The adult MS has a range of 5.0 to 22 ml with a mean volume of 12.5 ml and the mean length, width and height is 27.96 mm, 19.57 mm, and 25.33 mm, respectively [20, 21]. There is a negative correlation between age and distance to the meatus, mediolateral dimensions, and sinus volume, indicating a collapse of the maxillary bone over one's lifetime. Total MS volume is significantly smaller in completely or partially edentulous cases than in dentate cases [22].

Imaging

CBCT and conventional X-ray

The technique of the two-dimensional panoramic imaging was introduced in the first half of the 20th century, but the first device applying this technology was described in 1959 [23, 24]. It is especially useful in the initial diagnostic phase of the MSs to its pathologic conditions. However, it is well known that the images of the panoramic radiography (PA) are 1.25 times magnified on average. For the precise preoperative diagnosis when planning a lateral and internal sinus floor augmentation, precise assessment is mandatory [25, 26]. According to Malina-Altzinger et al. [24], there is a moderate risk for misdiagnosis of the MS if only the PA rather than CBCT is used, and resulted in different detection rate of the maxillary bone cysts penetrating into the sinus. Maestre-Ferrin et al. [14, 27] showed the PA led to false-positive and false-negative findings in the visualization of septa of the MS, and Krennmair et al. [11] observed the same inaccuracy of the PA in detecting the antral sinus septa in 13 out of 61 cases. Malina-Altzinger et al. [24] examined 54 MSs using CBCT, and the most frequent radiographic findings were basal septa (54 %), followed by basal opacities (43%), foreign bodies (15%). However, the result showed that there were no significant differences between PA and CBCT imaging methods for the detection of a complete opacity, a basal opacity, a foreign body, an oro-antral communication, a basal septum, a polypoid mucosal thickening, a fluid level, and a status post-SFA (Fig. 6). According to Toraman Alkurt et al. [28], the detection rate of the MS septa was 23.1% (24/104) on PA and 29.8% (31/104) on CBCT. Interestingly, of these, the MS septa on dentate posterior maxillary segment was detected in 10.6% (11/104) on PA, 19.2% (20/104) on CBCT.

CBCT studies showed that PSAA was detected in 61 to 87% of the patients; it was located underneath the mucosa in 22% to 47% (type I), intraosseus in 47% to 73% (type II) and

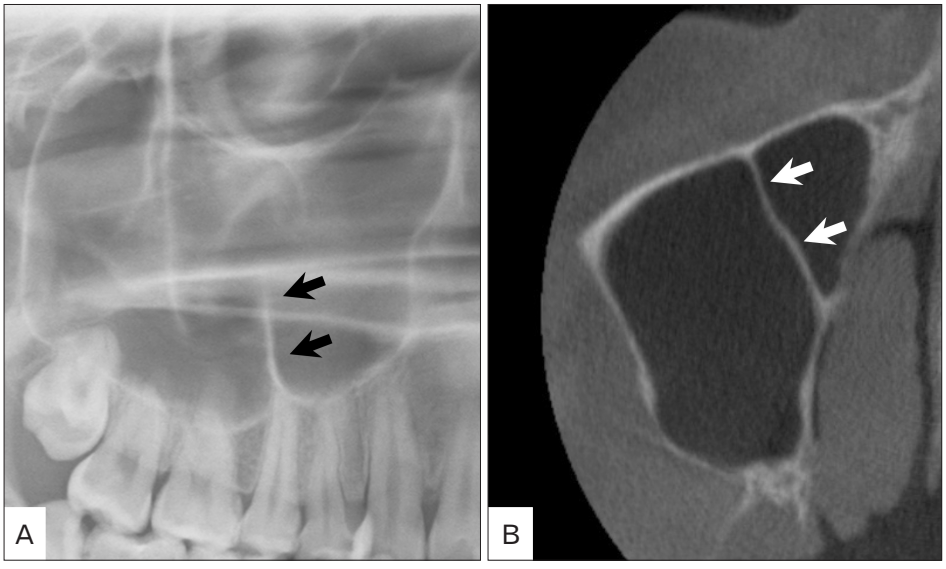

Fig. 6. Septum inside the right maxillary sinus (arrows). (A) Panoramic radiography. (B) Computed tomography (axial image).

https://doi.org/10.5115/acb.2019.52.1.17

external cortex (superficial) in 5% to 6% (type III), and the mean diameter of the PSAA was 0.63 mm to 1.37 mm [29-32]. According to Khojastehpour et al. [33], the rate of the detection rate of the PSAA in patients with an alveolar ridge height of <10 mm was significantly greater than the rate of detection in patients with an alveolar ridge height of >10 mm.

The artery was detected at a mean distance of 18 to 18.9 mm from the alveolar ridge in the edentulous region [10, 34]. According to Khojastehpour et al. [33], a mean distance from the alveolar ridge to the PSAA was 14.91 mm in females and 17.53 mm in males with a significant difference. While, Ilguy et al. [35] described that the mean distance between the artery and the alveolar ridge was 16.79 mm in females and 17.00 mm in males and there was no significant difference. In anatomical studies, this distance has been reported to be 18.9–19.6 mm [36, 37]. Water's X-ray is used for initial diagnosis for the MS lesion [38].

Magnetic resonance imaging

The main reason magnetic resonance imaging (MRI) used for the MS examination is to develop the treatment strategy and evaluate the tumor pre- and post-operatively [39, 40]. Many of them have done with CT analyses [41-43]. Only several researches were found on the PubMed in which the MRI was applied for SFA. Gray et al. [44] first described the use of MRI for the SFA in 1999 and concluded that images were good enough and should be considered as an alternative to the CT which exposes the patients to high dose of radiation. Gray et al. [45, 46] also investigated estimates of the bone graft volumes required for a desired vertical bone height preoperatively using MRI. Senel et al. [47] used the MRI to evaluate the vertical bone height after the SFA procedure. Thus, MRI has been applied for SFA in order to estimate or confirm the changes of the vertical bony height and avoid exposure for radiation. However, as shown in the small number of previous researches, the use of MRI has not achieved popularity for the SFA.

Endoscopy

The endoscopy has been mainly applied to transnasal removal of the dental implant [48-50], management of the perforating sinus membrane during the SFA [51]. Although some surgeons take advantage of endoscopy for experimental purposes [52], it has not been used extensively for dental implantology. According to Kunihiro et al. [53], the most important factor of the postoperative maxillary sinusitis after SFA is function of the natural ostium of the MS, and they proposed preoperative middle meatal antrostomy for the patient who will undergo SFA procedure when the patients do not have enough size of the ostium.

Conclusion

The anatomy of the MS is well understood due to many previous studies. However, the newly established surgical procedures and imaging devices require exact knowledge of the structures. Revisiting the classic anatomy and reviewing the newly published literature of the MS could help dentists perform safer surgery of the SFA.

References

1. Mavrodi A, Paraskevas G. Evolution of the paranasal sinuses' anatomy through the ages. Anat Cell Biol 2013;46:235-8.
2. Nuñez-Castruita A, López-Serna N, Guzmán-López S. Prenatal development of the maxillary sinus: a perspective for paranasal sinus surgery. Otolaryngol Head Neck Surg 2012;146:997-1003.
3. Standring S. Gray's anatomy: the anatomical basis of clinical practice. 41st ed. London: Elsevier Health Sciences; 2015.
4. Lang J. Clinical anatomy of the nose, nasal cavity, and paranasal sinuses. New York: Thieme Medical Publishers; 1989.
5. Duncavage J. The maxillary sinus: medical and surgical management. New York: Thieme Medical Publishers; 2011.
6. Chanavaz M. Maxillary sinus: anatomy, physiology, surgery, and bone grafting related to implantology: eleven years of surgical experience (1979-1990). J Oral Implantol 1990;16:199-209.
7. Eberhardt JA, Torabinejad M, Christiansen EL. A computed tomographic study of the distances between the maxillary sinus floor and the apices of the maxillary posterior teeth. Oral Surg Oral Med Oral Pathol 1992;73:345-6.
8. Kilic C, Kamburoglu K, Yuksel SP, Ozen T. An assessment of the relationship between the maxillary sinus floor and the maxillary posterior teeth root tips using dental cone-beam computerized tomography. Eur J Dent 2010;4:462-7.
9. Roque-Torres GD, Ramirez-Sotelo LR, Vaz SL, Bóscolo SM, Bóscolo FN. Association between maxillary sinus pathologies and healthy teeth. Braz J Otorhinolaryngol 2016;82:33-8.
10. Kim MJ, Jung UW, Kim CS, Kim KD, Choi SH, Kim CK, Cho KS. Maxillary sinus septa: prevalence, height, location, and morphology: a reformatted computed tomography scan analysis. J Periodontol 2006;77:903-8.
11. Krennmair G, Ulm CW, Lugmayr H, Solar P. The incidence, location, and height of maxillary sinus septa in the edentulous and dentate maxilla. J Oral Maxillofac Surg 1999;57:667-71.
12. Underwood AS. An inquiry into the anatomy and pathology of the maxillary sinus. J Anat Physiol 1910;44(Pt 4):354-69.
13. Lee WJ, Lee SJ, Kim HS. Analysis of location and prevalence of

maxillary sinus septa. J Periodontal Implant Sci 2010;40:56-60.
14. Maestre-Ferrín L, Carrillo-García C, Galán-Gil S, Peñarrocha-Diago M, Peñarrocha-Diago M. Prevalence, location, and size of maxillary sinus septa: panoramic radiograph versus computed tomography scan. J Oral Maxillofac Surg 2011;69:507-11.
15. Velásquez-Plata D, Hovey LR, Peach CC, Alder ME. Maxillary sinus septa: a 3-dimensional computerized tomographic scan analysis. Int J Oral Maxillofac Implants 2002;17:854-60.
16. González-Santana H, Peñarrocha-Diago M, Guarinos-Carbó J, Sorní-Bröker M. A study of the septa in the maxillary sinuses and the subantral alveolar processes in 30 patients. J Oral Implantol 2007;33:340-3.
17. Bell GW, Joshi BB, Macleod RI. Maxillary sinus disease: diagnosis and treatment. Br Dent J 2011;210:113-8.
18. Kqiku L, Biblekaj R, Weiglein AH, Kqiku X, Städtler P. Arterial blood architecture of the maxillary sinus in dentate specimens. Croat Med J 2013;54:180-4.
19. Flanagan D. Arterial supply of maxillary sinus and potential for bleeding complication during lateral approach sinus elevation. Implant Dent 2005;14:336-8.
20. Lovasova K, Kachlik D, Rozpravkova M, Matusevska M, Ferkova J, Kluchova D. Three-dimensional CAD/CAM imaging of the maxillary sinus in ageing process. Ann Anat 2018;218:69-82.
21. Gosau M, Rink D, Driemel O, Draenert FG. Maxillary sinus anatomy: a cadaveric study with clinical implications. Anat Rec (Hoboken) 2009;292:352-4.
22. Velasco-Torres M, Padial-Molina M, Avila-Ortiz G, García-Delgado R, O'Valle F, Catena A, Galindo-Moreno P. Maxillary sinus dimensions decrease as age and tooth loss increase. Implant Dent 2017;26:288-95.
23. Paatero YV. Orthoradial jaw pantomography. Ann Med Intern Fenn Suppl 1959;48(Supp 28):222-7.
24. Malina-Altzinger J, Damerau G, Grätz KW, Stadlinger PD. Evaluation of the maxillary sinus in panoramic radiography: a comparative study. Int J Implant Dent 2015;1:17.
25. Bornstein MM, Scarfe WC, Vaughn VM, Jacobs R. Cone beam computed tomography in implant dentistry: a systematic review focusing on guidelines, indications, and radiation dose risks. Int J Oral Maxillofac Implants 2014;29 Suppl:55-77.
26. Dula K, Benic GI, Bornstein M, Dagassan-Berndt D, Filippi A, Hicklin S, Kissling-Jeger F, Luebbers HT, Sculean A, Sequeira-Byron P, Walter C, Zehnder M. SADMFR guidelines for the use of cone-beam computed tomography/digital volume tomography. Swiss Dent J 2015;125:945-53.
27. Maestre-Ferrín L, Galán-Gil S, Carrillo-García C, Peñarrocha-Diago M. Radiographic findings in the maxillary sinus: comparison of panoramic radiography with computed tomography. Int J Oral Maxillofac Implants 2011;26:341-6.
28. Toraman Alkurt M, Peker I, Degerli S, Cebeci AR, Sadik E. Comparison of cone-beam computed tomography and panoramic radiographs in detecting maxillary sinus septa. J Istanb Univ Fac Dent 2016;50:8-14.
29. Tehranchi M, Taleghani F, Shahab S, Nouri A. Prevalence and location of the posterior superior alveolar artery using cone-beam computed tomography. Imaging Sci Dent 2017;47:39-44.
30. Chitsazi MT, Shirmohammadi A, Faramarzi M, Esmaieli F, Chitsazi S. Evaluation of the position of the posterior superior alveolar artery in relation to the maxillary sinus using the Cone-Beam computed tomography scans. J Clin Exp Dent 2017;9:e394-9.
31. Pandharbale AA, Gadgil RM, Bhoosreddy AR, Kunte VR, Ahire BS, Shinde MR, Joshi SS. Evaluation of the posterior superior alveolar artery using cone beam computed tomography. Pol J Radiol 2016;81:606-10.
32. Danesh-Sani SA, Movahed A, ElChaar ES, Chong Chan K, Amintavakoli N. Radiographic evaluation of maxillary sinus lateral wall and posterior superior alveolar artery anatomy: a cone-beam computed tomographic study. Clin Implant Dent Relat Res 2017;19:151-60.
33. Khojastehpour L, Dehbozorgi M, Tabrizi R, Esfandnia S. Evaluating the anatomical location of the posterior superior alveolar artery in cone beam computed tomography images. Int J Oral Maxillofac Surg 2016;45:354-8.
34. Güncü GN, Yildirim YD, Wang HL, Tözüm TF. Location of posterior superior alveolar artery and evaluation of maxillary sinus anatomy with computerized tomography: a clinical study. Clin Oral Implants Res 2011;22:1164-7.
35. Ilgüy D, Ilgüy M, Dolekoglu S, Fisekcioglu E. Evaluation of the posterior superior alveolar artery and the maxillary sinus with CBCT. Braz Oral Res 2013;27:431-7.
36. Solar P, Geyerhofer U, Traxler H, Windisch A, Ulm C, Watzek G. Blood supply to the maxillary sinus relevant to sinus floor elevation procedures. Clin Oral Implants Res 1999;10:34-44.
37. Traxler H, Windisch A, Geyerhofer U, Surd R, Solar P, Firbas W. Arterial blood supply of the maxillary sinus. Clin Anat 1999;12:417-21.
38. Maes JJ, Clement PA. The usefulness of irrigation of the maxillary sinus in children with maxillary sinusitis on the basis of the Water's X-ray. Rhinology 1987;25:259-64.
39. Eley KA, Watt-Smith SR, Boland P, Potter M, Golding SJ. MRI pre-treatment tumour volume in maxillary complex squamous cell carcinoma treated with surgical resection. J Craniomaxillofac Surg 2014;42:119-24.
40. Yuan XP, Li CX, Cao Y, Singh S, Zhong R. Inflammatory myofibroblastic tumour of the maxillary sinus: CT and MRI findings. Clin Radiol 2012;67:e53-7.
41. Ng SH, Chang TC, Ko SF, Yen PS, Wan YL, Tang LM, Tsai MH. Nasopharyngeal carcinoma: MRI and CT assessment. Neuroradiology 1997;39:741-6.
42. Asaumi J, Konouchi H, Hisatomi M, Kishi K. Odontogenic myxoma of maxillary sinus: CT and MR-pathologic correlation. Eur J Radiol 2001;37:1-4.
43. Yasumoto M, Taura S, Shibuya H, Honda M. Primary malignant lymphoma of the maxillary sinus: CT and MRI. Neuroradiology 2000;42:285-9.
44. Gray CF, Redpath TW, Smith FW, Staff RT, Bainton R. Assessment of the sinus lift operation by magnetic resonance imaging. Br J Oral Maxillofac Surg 1999;37:285-9.
45. Gray CF, Staff RT, Redpath TW, Needham G, Renny NM. As-

 https://doi.org/10.5115/acb.2019.52.1.17

sessment of maxillary sinus volume for the sinus lift operation by three-dimensional magnetic resonance imaging. Dentomaxillofac Radiol 2000;29:154-8.
46. Gray CF, Redpath TW, Bainton R, Smith FW. Magnetic resonance imaging assessment of a sinus lift operation using reoxidised cellulose (Surgicel) as graft material. Clin Oral Implants Res 2001;12:526-30.
47. Senel FC, Duran S, Icten O, Izbudak I, Cizmeci F. Assessment of the sinus lift operation by magnetic resonance imaging. Br J Oral Maxillofac Surg 2006;44:511-4.
48. Lim D, Parumo R, Chai MB, Shanmuganathan J. Transnasal endoscopy removal of dislodged dental implant: a case report. J Oral Implantol 2017;43:228-31.
49. Jeong KI, Kim SG, Oh JS, You JS. Implants displaced into the maxillary sinus: a systematic review. Implant Dent 2016;25:547-51.
50. Matti E, Emanuelli E, Pusateri A, Muniz CC, Pagella F. Transnasal endoscopic removal of dental implants from the maxillary sinus. Int J Oral Maxillofac Implants 2013;28:905-10.
51. Andreasi Bassi M, Andrisani C, Lico S, Ormanier Z, Barlattani A Jr, Ottria L. Endoscopic management of the schneiderian membrane perforation during transcrestal sinus augmentation: a case report. Oral Implantol (Rome) 2016;9:157-63.
52. Zheng J, Zhang S, Lu E, Yang C, Zhang W, Zhao J. Endoscopic lift of the maxillary sinus floor in Beagles. Br J Oral Maxillofac Surg 2014;52:845-9.
53. Kunihiro T, Araki Y, Oba T. Minimally invasive endoscopic middle meatal antrostomy for the prevention of maxillary sinusitis in association with dental implantation in the posterior maxilla: a proposal. Fukuoka Igaku Zasshi 2014;105:182-9.